JOURNAL OF MATERIALS SCIENCE 22 (1987) 547–553

Preparation and properties of nickel silicide layers by the diffusion and CVD processes using Si_2Cl_6 as a source of silicon

SEIJI MOTOJIMA, MASANORI KOHNO
Department of Industrial Chemistry, Faculty of Engineering, Gifu University, Gifu 501-11, Japan

TATSUHIKO HATTORI
Research Laboratory, Toagosei Chemical Industry Co. Ltd, 1-1 Funami-cho, Minato-ku, Nagoya 455, Japan

Nickel plate was siliconized with a gas mixture of Si_2Cl_6, H_2 and argon in the temperature range 400 to 900° C, and the siliconizing conditions and some of its properties were examined. Appreciable weight increase of the nickel plate was observed above 450° C, which is 200 to 300° C lower than that obtained using $SiCl_4$ as a source of silicon. Siliconizing of the surface and the resistance to high-temperature oxidation and hot corrosion were improved. Nickel silicide layers were also obtained by the CVD process using a gas mixture of Si_2Cl_6, $NiCl_2$, H_2 and argon.

1. Introduction

Nickel silicides have attracted considerable attention in recent years because of their potential applications in VLSI MOS devices [1], in photovoltaic solar cells [2], in catalysts for methanation [3, 4], gasification of coal [5] and smoke retardants [6], and in oxidation- and corrosion-resistant coatings for nickel- and iron-base superalloys, and for copper alloys [7, 8].

Ni–Si system alloys have been prepared by the direct synthesis process, melting the component metals in an induction furnace [1], and by the reaction of nickel with sodium silicate [9]. The nickel silicide layer has been most frequently formed on a silicon wafer by the deposition of nickel thin films on silicon, followed by the thermal or ion-beam annealing and interdiffusion of nickel with silicon (two-step processes) [10–16]. This process has been widely applied to prepare highly conductive composite gate structures for VLSI MOS devices [1]. Nickel silicide overlay coatings have also been prepared by electroless siliconizing [17], by ion implantation [18, 19], by the reaction sintering process with unalloyed powders [20], by a glow discharge process [21], and by the chemical vapour deposition (CDV) process [22, 23].

Diffusion coatings of metals with silicon have come to be used fairly widely in recent years to improve their physical and chemical properties, or to protect them against high-temperature oxidation and hot corrosion.

We have developed in recent years the commercial production process of hexachlorodisilane (Si_2Cl_6, b.p. 144° C). This new reagent has many advantages as a silicon source in the CVD or diffusion processes.

In this work, nickel plate, which is an important, and often the main, component of many superalloys, was siliconized using Si_2Cl_6 as a silicon source over a temperature range of 400 to 900° C, and some of its properties were examined. Silicon tetrachloride ($SiCl_4$, b.p. 57.6° C) was also used as a reference reagent. Furthermore, nickel silicide layers were also obtained by the CVD process using a gas mixture of Si_2Cl_6, $NiCl_2$, H_2 and argon.

2. Experimental procedure

2.1. Diffusion process

The nickel plate (8 mm × 8 mm × 0.5 mm) was set horizontally on a quartz boat which was located in the central part of the diffusion reaction tube (quartz, 22 mm i.d. × 150 mm long). The hexachlorodisilane was saturated into hydrogen gas using a bubble-type saturator, and was carried into the reaction tube.

2.2. CVD process

The CVD apparatus used for the deposition of nickel silicide layers from a gas mixture of Si_2Cl_6, $NiCl_2$, H_2 and argon is shown in Fig. 1. Nickel chloride was prepared *in situ* by the chlorination of nickel wire (0.6 mm diameter) at 800° C, and was introduced into the reaction tube. The graphite substrate (10 mm × 10 mm × 2 mm) was set slantingly on the susceptor.

2.3. Examination

The nickel silicide layer obtained was analysed by an X-ray diffractometer and energy-dispersive X-ray microanalyser (Akashi, EMAX-8000S). The Vickers microhardness of the siliconized layer was measured on the polished cross-section. The oxidation resistance of the siliconized nickel plate was characterized by the weight increase in an air atmosphere at a temperature of 700 to 1100° C for 2 h exposure time. The siliconized nickel

0022–2461/87 $03.00 + .12

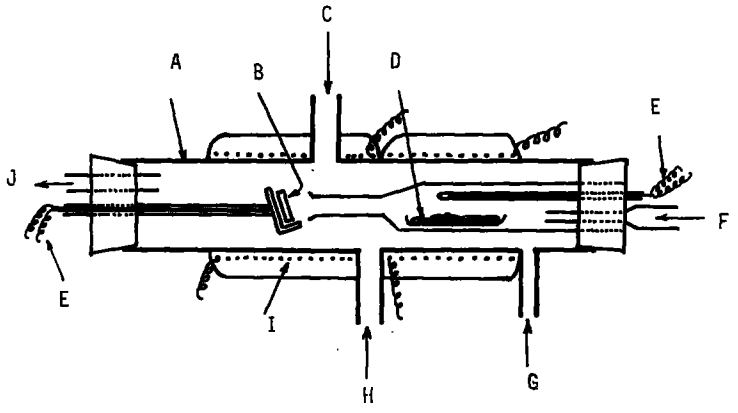

Figure 1 Apparatus used for the CVD process: (A) reaction tube (quartz, 22 mm i.d. × 200 long), (B) substrate (graphite, 10 mm × 10 mm × 2 mm), (C) H_2 inlet, (D) nickel wire (0.5 mm diameter), (E) chromel–alumel thermocouple, (F) Cl_2 + argon inlet, (G) argon inlet, (H) Si_2Cl_6 + H_2 inlet, (I) nichrome element, (J) gas outlet.

plate was immersed for 30 min into 1N sulphuric acid and 1N nitric acid solutions of 20 ml maintained at 100° C, and the weight decrease was examined.

3. Results and discussion

3.1. Preparation and properties of nickel silicide layers by the diffusion process

3.1.1. Deposition parameters

The effect of the silicon-source gas flow rate on the weight gain of the nickel plate is shown in Fig. 2, in which the reaction temperature and reaction time were fixed at 900° C and 60 min, respectively. With both silicon sources, the weight gains of the nickel plate increased with the same pattern with increasing flow rate of silicon source (Si_2Cl_6, $SiCl_4$), and attained a constant value at a rate above 0.015 ml sec^{-1} of Si_2Cl_6 or 0.03 ml sec^{-1} of $SiCl_4$. It can be seen that different effects of the sort of silicon-source gas, Si_2Cl_6 and $SiCl_4$, on the weight gain of the nickel plate are not observed at a reaction temperature of 900° C. In Region-A in Fig. 2, the rate-determining step for the siliconizing of the nickel plate was considered to be the gas-phase transport of reactant gas species and/or reaction of the species in the gas phase or on the surface of the nickel plate. On the other hand, that of Region-B was considered to be the diffusion of silicon or nickel atoms in the siliconized layers.

A distinct difference between Si_2Cl_6 and $SiCl_4$ on the siliconizing of nickel plate was observed at reaction temperatures above 900° C, as can be seen in Fig. 3. The effect of the reaction temperature on the weight gain for 60 min reaction time of nickel plate are shown in Fig. 3. In the case of Si_2Cl_6 at a flow rate of 0.013 ml sec^{-1}, the lowest appreciable weight gain was observed at a temperature above 450° C, and the weight gain increased exponentially with increasing reaction temperature. On the other hand, the lowest weight-gain temperature for $SiCl_4$ at flow rates of 0.071 and 0.018 ml sec^{-1} were above 650 and above 750° C, respectively. It can be seen that by using Si_2Cl_6 as a silicon source in place of $SiCl_4$, which has been commonly used as a silicon source in the diffusion process, the siliconizing temperature of nickel plate is lowered by 200 to 300° C. This outstanding effect of Si_2Cl_6 on the siliconizing temperature may probably be attributed to the higher reactivity of Si_2Cl_6 than that of $SiCl_4$, leading to the abundant formation of highly active species at lower temperatures.

The weight gain was affected appreciably by the source-gas ratio (H/Cl), and the weight gain decreased noticeably below and above the ratio H/Cl = 20 at which maximum weight gain was attained.

3.1.2. Morphology of the siliconized layers

The siliconized surface of the nickel plate was composed of fine-grained particles at a low reaction temperature, but was roughened by the growth of the silicide layers in the vertical direction with increasing

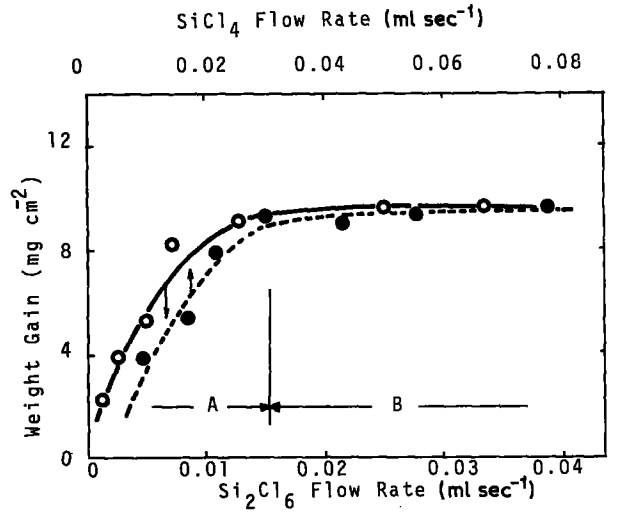

Figure 2 Effect of Si_2Cl_6 and $SiCl_4$ flow rates on the weight gain. Reaction temperature 900° C, reaction time 60 min, total gas flow rate 2.6 ml sec^{-1}, H_2 flow rate 0.65 ml sec^{-1}. (○) Si_2Cl_6, (●) $SiCl_4$.

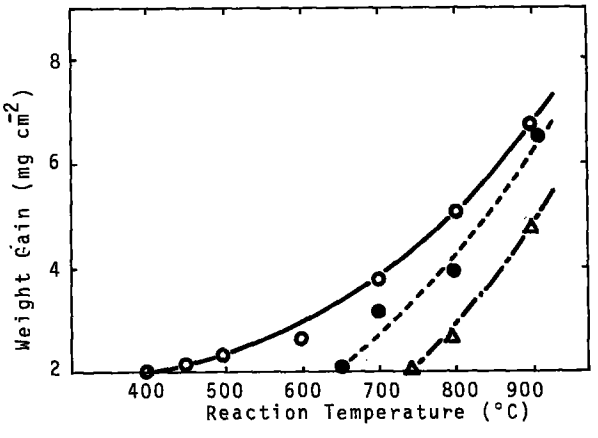

Figure 3 Effect of the reaction temperature on the weight gain. Reaction time 60 min, total gas flow rate 2.6 ml sec^{-1}, H_2 flow rate 0.65 ml sec^{-1}. (○) Si_2Cl_6 flow rate: 0.013 ml sec^{-1}, (△) $SiCl_4$ flow rate 0.018 ml sec^{-1}, (●) $SiCl_4$ flow rate 0.079 ml sec^{-1}.

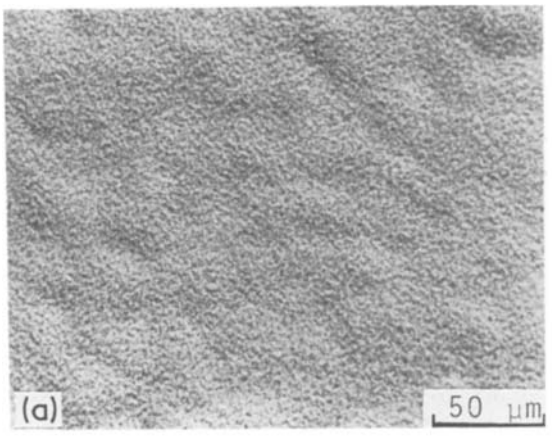

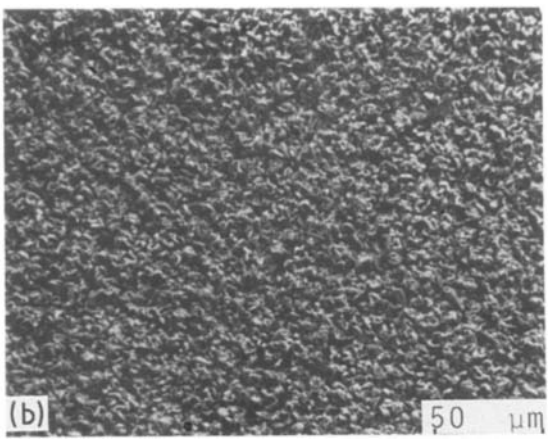

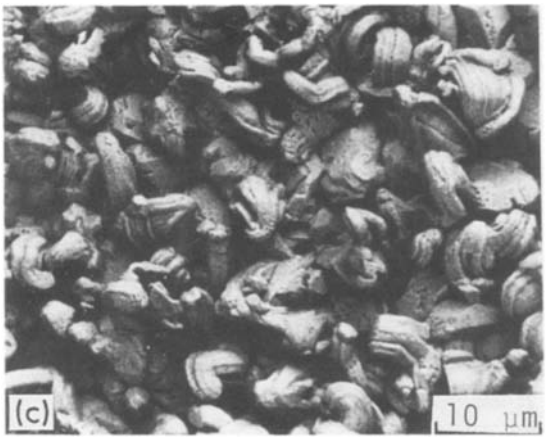

Figure 4 Surface appearances of the siliconized nickel plate. Reaction temperature: (a) 600° C, (b) 900° C, (c) 900° C. Reaction time 60 min, total gas flow rate 2.60 ml sec^{-1}, Si_2Cl_6 flow rate 0.026 ml sec^{-1}, H_2 flow rate 0.65 ml sec^{-1}.

reaction temperature, as can be seen in Fig. 4. An enlarged view of the characteristic morphology of the surface of siliconized layers obtained at 900° C is shown in Fig. 4c. An influence of the sort of silicon source on the surface morphology was not observed.

A polished cross-section of the siliconized layer is shown in Fig. 5. It has been found that the dominant species during the formation of the silicide layer by the interdiffusion of nickel and silicon thin layers is the nickel atom, and that it moves predominantly by grain-boundary diffusion or by interstitial diffusion [12]. Many of the voids or cavities found in the siliconized layer would be formed by the faster diffusion velocity of nickel atoms from the nickel plate to the surface of the siliconized layer, compared with that of silicon atoms from the surface of the siliconized layer to the interface of the siliconized layer and the nickel plate.

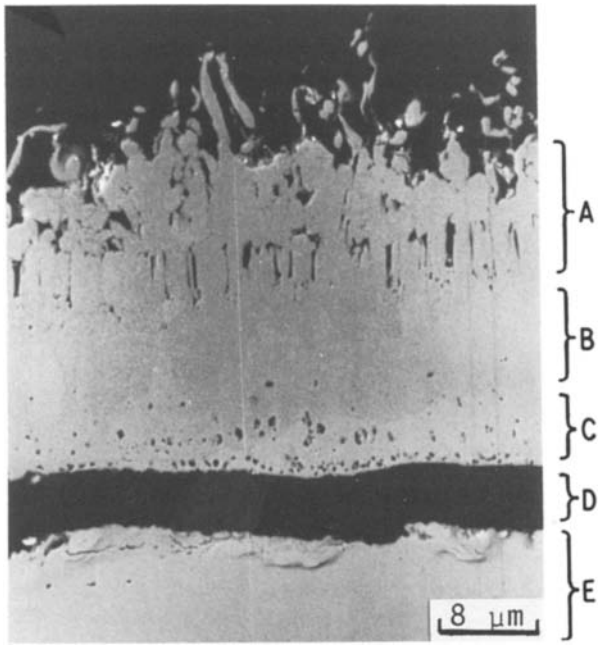

Figure 5 Cross-section of the siliconized nickel plate. Reaction temperature 900° C. (A) Ni_3Si_2 layer, (B) Ni_2Si layer, (C) Ni_5Si_2 layer, (D) crack, (E) nickel plate.

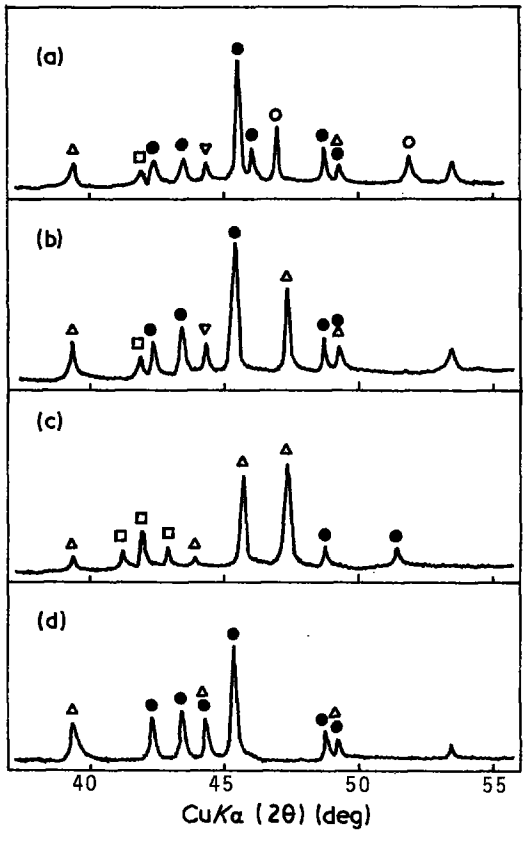

Figure 6 X-ray diffraction patterns from the surface of the siliconized nickel plate. Reaction temperature: (a) 600° C, (b) 700° C, (c) 800° C, (d) 900° C. (○) Ni_3Si_2, (●) ε-Ni_3Si_2, (□) Ni_5Si_2, (△) σ-Ni_2Si, (▽) ζ-$NiSi_2$. Total gas flow rate 2.6 ml sec^{-1}, Si_2Cl_6 flow rate 0.026 ml sec^{-1}, H_2 flow rate 0.65 ml sec^{-1}.

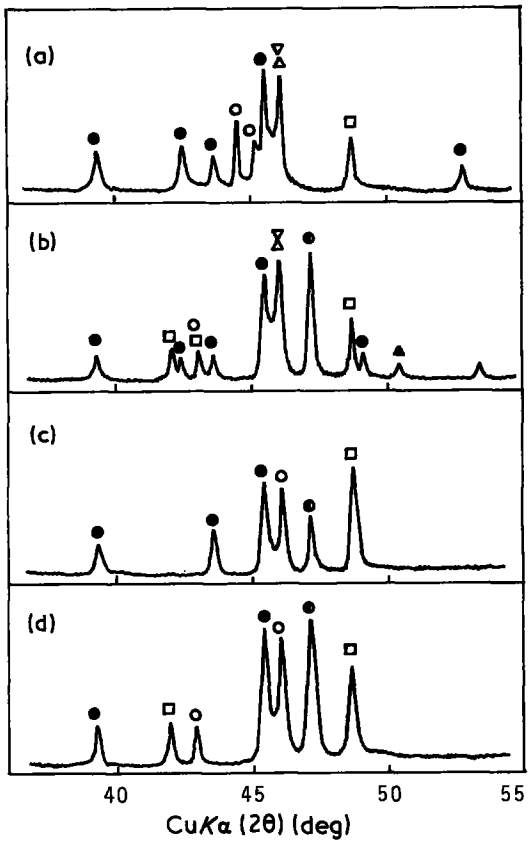

Figure 7 X-ray diffraction patterns from the back side of the siliconized nickel plate. Reaction temperature: (a) 600° C, (b) 700° C, (c) 800° C, (d) 900° C. (○) Ni_3Si_2, (●) ε-Ni_3Si_2, (□) Ni_5Si_2, (△) σ-Ni_2Si, (▽) ζ-$NiSi_2$, (◐) θ-Ni_2Si, (▲) η-NiSi.

3.1.3. X-ray analysis of the siliconized layers

Representative X-ray diffraction patterns of the surface of the siliconized layers using Si_2Cl_6 are shown in Fig. 6. Mixed peaks of Ni_3Si_2, ε-Ni_3Si_2, σ-Ni_2Si and Ni_5Si_2 can be seen irrespective of the reaction temperature. The main component of the surface of the siliconized layer is considered to be ε-Ni_3Si_2. The thick siliconized layer can be readily stripped from the nickel plate. X-ray diffraction patterns of the inner surface of the stripped layers are shown in Fig. 7. Many peaks assigned to the respective nickel silicide phases can be seen, and the main components cannot be determned at any reaction temperature. However, the presence of the Ni_5Si_2 phase, which is the high-nickel phase and is rarely observed on the outer surface, was observed at all reaction temperatures. The coexistence and simultaneous growth of many nickel silicide phases such as NiSi, Ni_2Si, Ni_3Si and Ni_5Si, have been reported for silicide formation in bulk couples [24], but the presence of Ni_3Si and Ni_5Si phases were not observed in this experiment.

X-ray microanalysis was carried out on a cross-section of siliconized layers 50 μm thick obtained at 900° C. In Fig. 8, the peak area ratio (Si*Kα*/Ni*Kα*) is shown as a function of the separation from the boundary with the nickel plate. It can be seen that the peak ratio (Si*Kα*/Ni*Kα*) increases linearly with increasing separation. The polished cross-section shown in Fig. 5 reveals the existence of three appreciable layers. It may reasonably be considered from these results that the main component of the respective layers changes from the inner to outer layers as Ni_5Si_2, Ni_2Si, Ni_3Si_2.

3.1.4. Some properties of the siliconized nickel plate

3.1.4.1. Microhardness. The Vickers microhardness of the cross-section of the siliconized layer is shown in Fig. 8, in which the indentation load was 100 g. The microhardness decreased linearly with the separation from the boundary with the nickel plate. This tendency is inversely proportional to that of the silicon ratio (Si*Kα*/Ni*Kα*) in the layers.

3.1.4.2. Corrosion resistance. The corrosion resistance of the siliconized nickel plate against 1N sulphuric acid and 1N nitric acid is shown in Fig. 9, in which the nickel plate was siliconized at 900° C using Si_2Cl_6 as a silicon source. The weight decrease of the siliconized nickel plate caused by 1N nitric acid corrosion decreased exponentially with increasing thickness of the siliconized layer, and the weight decrease was as low as below 1 wt% at a thickness above 50 μm. Nickel plate is outstandingly unstable against nitric acid, and 50 wt% loss was observed after 30 min immersion time in 1N nitric acid at 100° C. Thus, is may be concluded that the corrosion resistance of the nickel plate against nitric acid is outstandingly improved by the siliconizing of the surface. On the other hand, the corrosion resistance of the nickel plate against 1N sulphuric acid was reduced by the siliconizing of the surface.

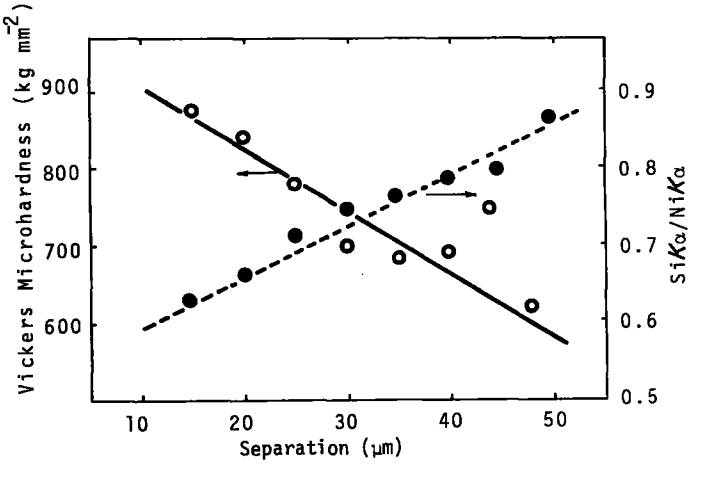

Figure 8 Vickers microhardness and peak ratio (Si*Kα*/Ni*Kα*) from X-ray microanalysis. Reaction temperature 900° C, thickness of the silicide layers 50 μm, total gas flow rate 2.6 ml sec^{-1}, H_2 flow rate 0.65 ml sec^{-1}, Si_2Cl_6 flow rate 0.026 ml sec^{-1}. Indentation load 100 g. (○) Microhardness, (●) Si*Kα*/Ni*Kα*.

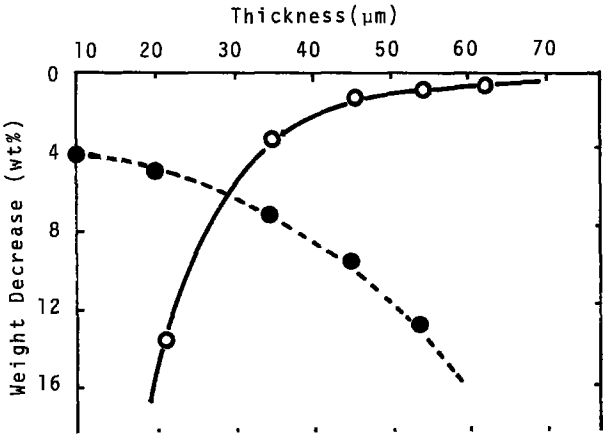

Figure 9 Corrosion stability of the siliconized nickel plate against 1N H_2SO_4 and 1N HNO_3. Reaction temperature 900° C, total gas flow rate 2.6 ml sec^{-1}, H_2 flow rate 0.65 ml sec^{-1}, Si_2Cl_6 flow rate 0.026 ml sec^{-1}. Immersion conditions in 1N H_2SO_4 or 1N HNO_3: temperature 100° C, time 30 min. (●) 1N H_2SO_4, (○) 1N HNO_3.

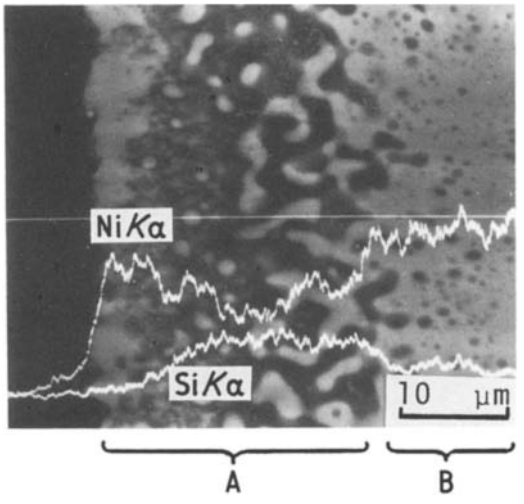

Figure 11 Cross-section of the siliconized nickel plate when exposed in air at 1100° C. Reaction temperature 800° C; (A) oxidized layer, (B) nickel silicide layers.

3.1.4.3. Oxidation resistance. Siliconized nickel plates with a silicide layer 50 μm thick were exposed in an air atmosphere at high temperature for 2 h and the weight increase is shown in Fig. 10, with that of the bare nickel plate as a reference sample. The bare nickel plate begins to be oxidized at a temperature of about 600° C, and oxidized outstandingly above 1000° C. Using Si_2Cl_6 as a silicon source, a weight increase of the siliconized nickel plate was not observed at all at a temperature of 700° C, and the weight increased gradually at a temperature above 700° C at a fifth of that of bare nickel plate and a half of the siliconized nickel plate using $SiCl_4$ as a silicon source. That is, the oxidation resistance of the nickel plate is improved oustandingly by the siliconizing of the surface using Si_2Cl_6.

No influence of the reaction temperature on the oxidation resistance of the siliconized nickel plate was observed over a reaction temperature range of 500 to 900° C, and the same weight increase was observed.

The surface of the oxidized layer was very dense and of a greenish colour, and the presence of an NiO phase was identified by X-ray diffraction on the surface of the oxidized layer. A polished cross-section of oxidized siliconized nickel plate is shown in Fig. 11, in which a siliconized nickel plate was exposed in an air atmosphere for 2 h at 1100° C. The silicon content of the surface of the oxidized layer (A in Fig. 11) is much lower than that of the siliconized layer (B in Fig. 11), and is nearly zero. It can be seen that nickel silicides are present as islands in the oxidized inner layers. It has been reported that nickel silicides, such as $NiSi_2$, are oxidized parabolically in time to form an outer-surface SiO_2 layer [25]. In this experiment, however, no obvious SiO_2 single-phase surface layer was observed, as can be seen in Fig. 11. The inner oxidized layer (A in Fig. 11) is considered to be composed of mixed phases of SiO_2 and NiO.

3.2. Preparation of nickel silicides by the CVD process using Si_2Cl_6 as a silicon source

Various phases of the nickel silicides were deposited on a graphite substrate from a gas mixture of Si_2Cl_6–$NiCl_2$–H_2–Ar over a temperature range of 800 to 1100° C. A CVD phase diagram in relation to the deposition temperature and source gas ratio (Ni/Si) is shown in Fig. 12. A single phase of Ni_3Si_2 was

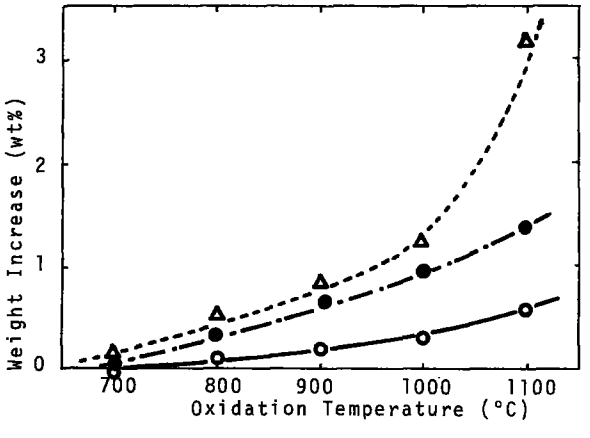

Figure 10 Oxidation stability of the siliconized nickel plate. Reaction temperature 900° C, thickness of the silicide layers 50 μm, total gas flow rate 2.6 ml sec^{-1}, H_2 flow rate 0.065 ml sec^{-1}, Si_2Cl_6 flow rate 0.026 ml sec^{-1}, $SiCl_4$ flow rate 0.052 ml sec^{-1}. (△) Bare nickel plate. Silicon source: (○) Si_2Cl_6, (●) $SiCl_4$.

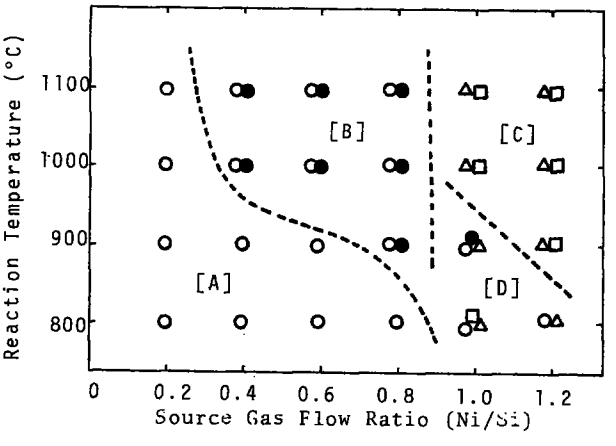

Figure 12 Composition of the deposits obtained by the CVD process: (○) Ni_3Si_2, (●) ε-Ni_3Si_2, (△) σ-Ni_2Si, (□) Ni_5Si_2.

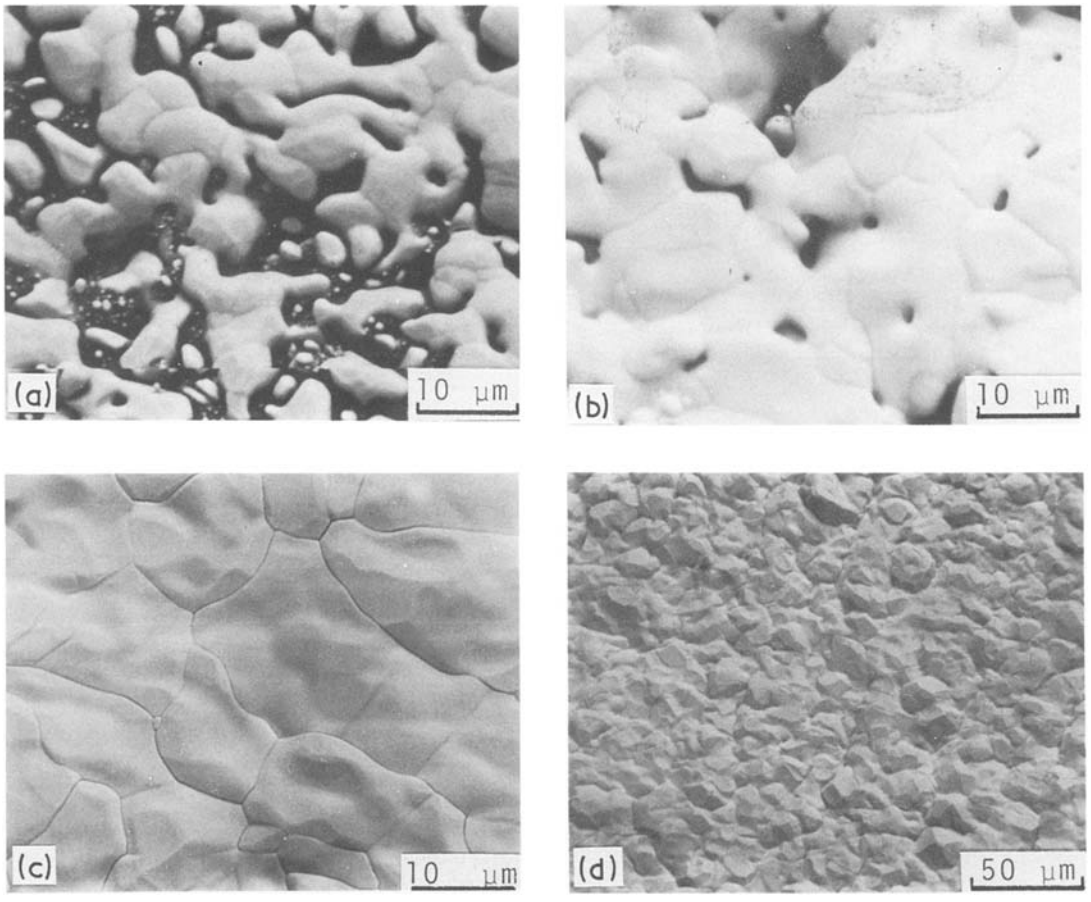

Figure 13 Morphologies of the Ni_3Si_2 deposits obtained by the CVD process. Reaction temperature: (a to c) 1000° C, (d) 1100° C. Reaction time 30 min. Si_2Cl_6 flow rate: (a to c) 0.063 ml sec^{-1}, (d) 0.022 ml sec^{-1}. $NiCl_2$ flow rate: (a to c) 0.026 ml sec^{-1}, (d) 0.034 ml sec^{-1}.

deposited at a relatively low deposition temperature and low source gas ratio (Ni/Si) (Region-A in Fig. 12). Mixed phases of Ni_3Si_2 and ε-Ni_3Si_2 were obtained over the temperature range 1000 to 1100° C and a gas flow ratio (Ni/Si) of 0.4 to 0.8. High nickel-content phases of Ni_2Si or Ni_5Si_2 were deposited at a ratio (Ni/Si) above 1.0.

Surface morphologies of the Ni_3Si_2 single phase deposited at 1000° C and a ratio (Ni/Si) of 0.2 are shown in Fig. 13. Ni_3Si_2 deposits were formed as islands on the graphite substrate in the initial stage of deposition, followed by infiltration of the open space to form uniform layers as can be seen in Fig. 13c.

Well-crystallized Ni_3Si_2 deposits with many crystal facets on the surface were obtained at 1100° C (Fig. 13d). A single crystal of hexagonally shaped Ni_3Si_2 was observed frequently on the layers (Fig. 14a). Coral-like deposits were sometimes observed on the edge of the graphite substrate (Fig. 14b).

References

1. D. B. FRASER, E. KINSBRON and F. VRATNY, US Patent 4 362 597 (1983).
2. R. GONSIORAWSKI and K. B. PATEL, UK Patent Application, GB 2 107 741 (1983) (*Chem. Abstr.* **99** (1983) 9528e).
3. M. HOUALLA, C. L. KIBBY, L. PETRAKIS and

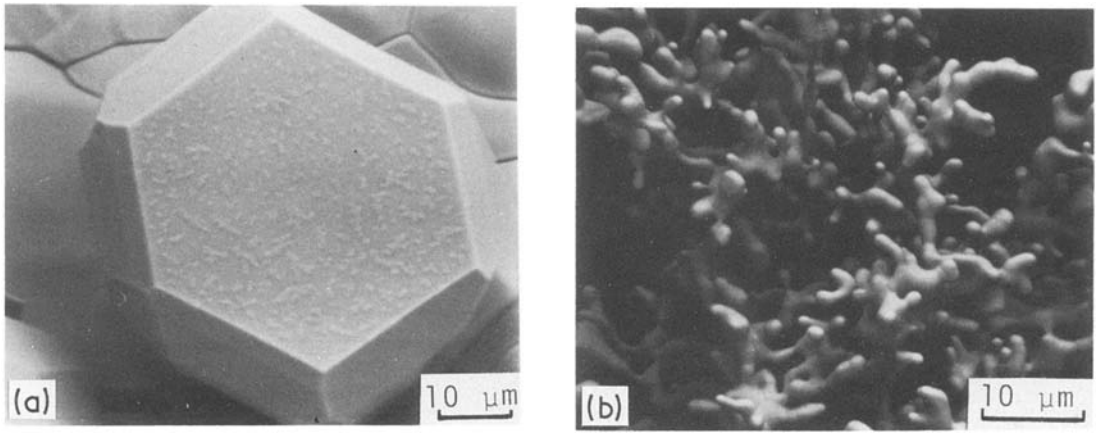

Figure 14 Morphologies of the Ni_3Si_2 deposits obtained by the CVD process. Reaction temperature 1000° C, Si_2Cl_6 flow rate 0.063 ml sec^{-1}, $NiCl_2$ flow rate 0.051 ml sec^{-1}. (a) Ni_3Si_2 single crystal deposited on the central part of the substrate; (b) Ni_3Si_2 dendrites deposited on the rim of the substrate.

D. M. HERCULES, *J. Phys. Chem.* **87** (1983) 3689.
4. H. IMAMURA and W. E. WALLACE, *ibid.* **83** (1979) 2009.
5. A. M. LEAS, US Patent 4167615 (1979).
6. E. D. DICKENS Jr, US Patents 3968064 (1976), 3975359 (1976).
7. E. FITZER, H. J. MAEURER, W. NOWAK and J. SCHLICHTING, *Thin Solid Films* **64** (1979) 305.
8. A. M. BELTRAN, N. R. LINDBLAD and G. E. WASIELEWSKI, US Patent 3904328 (1976).
9. A. A. APPEN, N. S. ANDRUSHCHENKO, I. B. BAŃKOVSKAYA and M. V. SAZONOVA, *Fiz. Khim. Obrab. Mater.* **6** (1972) 51 (*Chem. Abstr.* **78** (1973) 86625c).
10. K. N. TU, E. I. ALESSAUDRINI, W. K. CHU, H. KROÜTLE and J. W. MAYER, *Jpn. J. Appl. Phys.* **13** Suppl. 2, Part 1 (1974) 669.
11. T. G. FINSTAD, J. W. MAYER and M-A. NICOLET, *Thin Solid Films* **51** (1978) 391.
12. R. PRETORIUS, C. L. RAMITTER, S. S. LAU and M-A. NICOLET, *Appl. Phys. Lett.* **30** (1977) 501.
13. J. E. E. BAYLIN, H. A. ATWATER, D. GUPTA and F. M. D'HEURLE, *Thin Solid Films* **93** (1982) 255.
14. A. I. RODIONOV and V. A. USKOV, *Izv. Vyssh. Uchebn. Zaved. Fiz.* **28** (1985) 78 (*Chem. Abstr.* **102** (1985) 226315t).
15. B. L. MEILER, *Poverkhnost* **4** (1985) 67 (*Chem. Abstr.* **102** (1985) 195982b).
16. L. J. CHEN, L. S. HUNG, J. W. MAYER, J. E. E. BAGLIN, J. M. NERI and D. A. HAMMER, *Appl. Phys. Lett.* **40** (1982) 595.
17. A. J. GAY and J. QAUKERNAAT, *J. Less-Common Metals* **40** (1975) 21.
18. K. HIKOSAKA, H. ISHIWARA and S. FURUKAWA, *J. Vac. Sci. Technol.* **16** (1979) 1913.
19. V. YU. PETUKHOV, I. B. KHAIBULLIN and M. M. ZARIPOV, *Poverkhnost* **2** (1985) 104.
20. E. FITZER, H. J. MAEURER, W. NOWAK and J. SCHLICHTING, *Thin Solid Films* **64** (1979) 305.
21. M. SOKOLOWSKI, A. SOLOLOWSKA, E. ROLINSKI and A. MICHALSKI, *ibid.* **30** (1975) 29.
22. D. ITZHAK, F. R. TULER and M. SCHIEBER, *ibid.* **73** (1980) 379.
23. A. OLSEN and F. R. SALE, *Met. Technol.* **7** (1980) 494 (*Chem. Abstr.* **94** (1981) 196446h).
24. K. N. TU, G. OTTAVIANI, U. GOSELE and H. FOLL, *J. Appl. Phys.* **54** (1983) 758.
25. M. BARTUR and M-A. NICOLET, *ibid.* **54** (1983) 5404.

Received 18 March
and accepted 2 June 1986